# Whole-Rock K-Ar Model and Isochron, and Rb-Sr, Sm-Nd, and Pb-Pb Isochron, "Dating" of the Somerset Dam Layered Mafic Intrusion, Australia

**Andrew A. Snelling**, PhD,

Institute for Creation Research, PO Box 2667, El Cajon, California, 92021, USA.*

*current address: Answers in Genesis, PO Box 510, Hebron, Kentucky, 41048, USA.

*Presented at the Fifth International Conference on Creationism, Pittsburgh, Pennsylvania, August 4–9, 2003. Published in:* Proceedings of the First International Conference on Creationism, *R. L. Ivey (Eds.), pp. 305–324, 2003.*



**Abstract**

The Somerset Dam layered mafic intrusion in southeast Queensland, Australia, has been conventionally dated as Late Triassic by the apparently successful application of radioisotopic dating techniques. Mineralogical, geochemical, and isotopic evidence indicates that all of this gabbro intrusion's cyclic units were derived coevally from the same parental basaltic magma, with an initial homogeneous isotopic mixture ideal for yielding concordant isochron ages. However, newly obtained K-Ar, Rb-Sr, Sm-Nd, and Pb-Pb radioisotopic data from 15 whole-rock samples (representing all gabbro macrolayers in four of the intrusion's cyclic units) yield discordant isochron "ages," although the excellent-fitting 15-point K-Ar isochron suggests the resultant 174±8Ma "age" (Middle Jurassic) should be regarded as the revised conventional age of the layered intrusion. Nevertheless, it is concluded that these discordances between the radioisotope systems are likely due to changes in their decay rates in the past, with the longer half-life β-emitter $^{87}Rb$ being accelerated more and thus yielding an older "age." Furthermore, the Sr, Nd, and Pb isotopes indicate the parental basaltic magma was derived from a depleted mantle source, while the large spread of Nd $T_{DM}$ "ages" suggests accelerated radioisotopic decay rates during the partial melting and magma ascent. It is concluded that the Somerset Dam layered mafic intrusion has inherited the radioisotopic signature of its mantle source, and so the conventional radioisotopic dating techniques do not provide its true age.

**Keywords**

Gabbro, Layered Intrusion, Australia, Potassium-Argon, Rubidium-Strontium, Samarium-Neodymium, Lead-Lead, Radioisotopic Dating, Whole-Rock Model "Ages," Whole-Rock Isochron "Ages," Discordances, Decay "Constants," Accelerated Decay, Mantle Source Inheritance

## Introduction

The Somerset Dam layered mafic intrusion is situated immediately west of the village of Somerset Dam at 152°32'E and 27°7'S, some 65km northwest of the city of Brisbane in south-east Queensland on Australia's east coast (Figure 1). The outcrop is somewhat oval shaped, covering an area of about 4km$^2$ with a diameter of about 1.5km. It is a small layered gabbro intrusion with an exposed stratigraphic thickness of 500m on a steep hillside. It is a well-preserved, well-exposed, steep-sided, discordant intrusion which is undeformed and unmetamorphosed. The roof and floor of the intrusion are not exposed, and unknown thicknesses of the layered gabbros of the intrusion have been eroded from the top, and are concealed below the exposed sequence. The location and nature of the feeder zone are unknown, yet it probably represents a small, relatively shallow (3–5km depth), subvolcanic magma chamber (Mathison, 1967, 1987).

Due to its relatively small size, excellent preservation and good exposure this layered gabbro intrusion is ideal for the study of the physical and chemical processes occurring in magma chambers emplaced at shallow crustal depths below volcanos and feeding them. Indeed, layered mafic intrusions provide valuable information on the processes effecting magmas while they are transported from their mantle sources until they are emplaced. The Somerset Dam intrusion though is fundamentally different from the classic Skaergaard intrusion in Greenland (McBirney & Noyes, 1979; Wager & Brown, 1968) and the giant Bushveld Complex intrusion in South Africa (Wager, Brown, & Wadsworth, 1960; Zingg, 1996), since it is characterized by several repetitions of similar patterns, and progressive differentiation is absent, suggesting venting of the magma chamber through the overlying volcano and recharge from the magma source below several times during its emplacement and cooling. The age of this intrusion and the timing

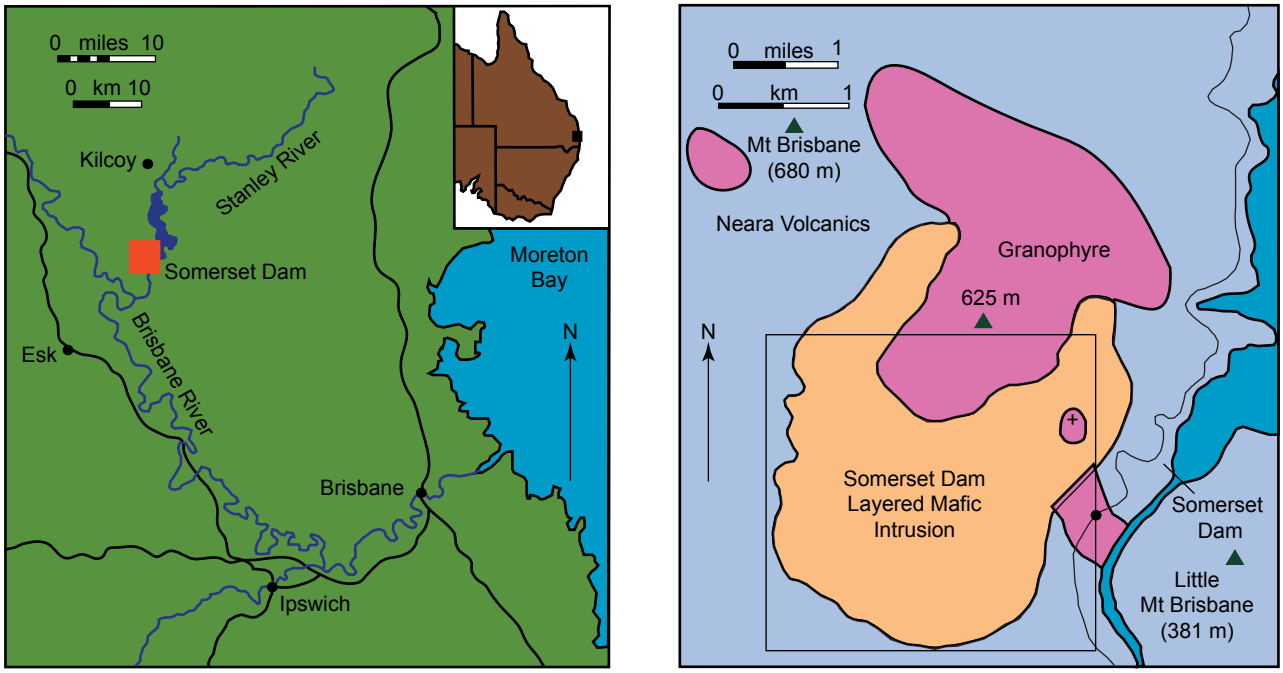


**Figure 1.** Location and general geology maps for the Somerset Dam layered mafic intrusion (after Mathison, 1967).

of these processes have to be younger than the andesitic lavas that the magma body has intruded, so radioisotope dating has been the only means for determining some time constraints.

## Geologic Setting

The Somerset Dam layered mafic complex intrudes the andesitic lavas and tuffs of the Neara Volcanics, which have been dated as early Middle Triassic based on plant spores in the underlying and overlying sedimentary formations (Cranfield, Schwartzbock, & Day, 1976), and on radioisotope dates of 240±11Ma (Ar-Ar), 232Ma and 242±8Ma (K-Ar) (Cranfield et al; Day, Whittaker, Murray, Wilson, & Grimes 1975; Murphy, Schwarzbock, Cranfield, Withnall, & Murray, 1976). Together with other acid to intermediate volcanics and volcaniclastic and clastic sediments, the Neara Volcanic were deposited in the downfaulted Esk Trough, a Mesozoic basin within the Paleozoic New England Orogen, elongated blocks of which are exposed to the west and east paralleling the sides of the Esk Trough (Flood & Aitchison, 1993; Harrington & Korsch, 1985). To the south, the sediments and volcanics of the Esk Trough plunge beneath the clastic sediments and coal seams of the Upper Triassic–Jurassic Moreton Basin.

The region is characterized by younger basaltic volcanism, radioisotope dated as Late Oligocene to Early Miocene (Day et al, 1983; Webb, Stevens, & McDougall, 1967). These volcanic rocks form a continuous belt extending north-northwest from near the coast south of Brisbane for over 200km parallel and close to the mountains west of the Brisbane River Valley, which has been eroded into the sediments and volcanics of the Esk Trough. This volcanism produced large, now eroded, shield volcanoes, complex lava fields, ring complexes and localized cones, plugs, laccoliths, sills and dikes (Ewart & Grenfell, 1985). Other Tertiary volcanic remnants are found outcropping to the east and northeast of the Somerset Dam intrusion, perhaps suggesting a wider distribution of these lava flows across the region prior to the erosion.

The geological development of the region has been carefully documented by Cranfield et al. (1976). Based on stratigraphic relationships, the Somerset Dam layered gabbro intrusion is clearly younger than the Neara Volcanics it intrudes, but just how much younger has only been determined by radioisotopic dating which has yielded Late Triassic ages for the intrusion (Walker, 1998; Webb & McDougall, 1967). Nevertheless, if it were not for conventional biostratigraphic and radioisotopic dating a genetic relationship between the Somerset Dam gabbro and the basaltic volcanism which produced the Tertiary shield volcanoes and lava fields may not be excluded. According to stratigraphic relationships, the sediments of the Moreton Basin overly the Neara Volcanics and other sediments of the Esk Trough, with the erosion of both these basins apparently commencing prior to the extrusion of the basalt and related lavas of the shield volcanos and lava fields (Begemann, Ludwig, Lugmair, Min, Nyquist, Latchett, Renne, Shih, Villa, & Walker, 2001; Ollier, 1982). However, an interpretation of the regional geologic record within a biblical framework and timescale would place the deposition of the volcanics

and sediments in these Mesozoic basins as late in the Flood year, with the subsequent erosion at the end of the Flood and extending into the post-Flood era to the present day. Thus if the Tertiary basaltic volcanic activity occurred early in the post-Flood era, then it would not be far removed in time, or spatially, from the Somerset Dam gabbro intrusion that has been interpreted as the remains of the magma chamber feeding a basaltic volcano.

## Geology of the Intrusion

The geology of the Somerset Dam layered mafic intrusion and its immediate area has been thoroughly mapped and investigated (Mathison, 1964, 1970; McLeod, 1956, 1959; Riley, 1991; Walker, 1998; Walsh, 1972). The general geology of the immediate area is shown in Figure 1, while Figure 2 provides a detailed geologic map and appropriate cross-sections of the intrusion, based on the definitive work of Mathison (1964, 1967, 1970).

Within this gabbro intrusion there is an exposed sequence of 22 saucer-shaped macrolayers, 3–50 m thick generally dipping inwards at 10–20°. The contacts between these prominent layers are sharply defined, generally to within 10 cm, and are phase, modal mineralogy and textural contacts. These macrolayers appear to be stratigraphically and laterally homogeneous. The repetition of these macrolayers has allowed the recognition of at least six well-developed cyclic units, ranging from 30 to 150 m thick (average about 80 m thick). The macrolayers are limited to only four main rock types, which are defined in terms of their essential cumulus mineral phases (distinguished texturally from the intercumulus mineral phases) (Irvine, 1982; Wager, Brown, & Wadsworth, 1960). These four rock types constituting the macrolayers are leucogabbro or anorthosite (plagioclase cumulate), troctolite (plagioclase + olivine cumulate), olivine gabbro (plagioclase + augite + olivine cumulate), and oxide (or ferri-) gabbro (plagioclase + augite ± olivine + magnetite + ilmenite cumulate).

The definition of these cyclic units, selecting which of these macrolayers commences each cycle, is somewhat interpretive. The choice is strongly influenced by what is expected to be the order of crystallization and the magma fractionation pattern, because there is commonly no clear field evidence to identify the base and top of a cyclic unit. In the Somerset Dam gabbro intrusion, Mathison (1964, 1967, 1970, 1975) chose to define each cyclic unit to be the sequence troctolite–olivine gabbro–oxide gabbro–leucogabbro, because troctolite was considered the least fractionated rock type, and cryptic trends generally suggested a reversal at the bases of the troctolites. However, Mathison (1987) revised this choice of sequence in each cyclic unit so that anorthosite was defined as the basal layer and oxide gabbro as the top layer in each cyclic unit, the choice subsequently followed by Walker (1998). This interpretation better fits the inferred order of crystallization, the oxide gabbro being the most fractionated rock type. Mineral compositions in a typical cyclic unit therefore show a reversed fractionation trend in the sequence from anorthosite to troctolite, and a normal fractionation trend from troctolite through olivine gabbro to oxide gabbro (Mathison, 1967, 1987). Whole-rock compositions also show marked changes between these rock types in this cyclical sequence (Mathison, 1967, 1987; Walker, 1998).

Despite the remarkable similarity of successive cyclic units, significant differences exist between them in the sequences of macrolayers, thicknesses of individual macrolayers and of the cyclic units, mineral compositions and cryptic patterns, average level of fractionation, and the sizes of the reversals (Mathison, 1967, 1970, 1975, 1987). Figure 3 shows the stratigraphic sequence in macrolayers within the Somerset Dam intrusion, with the cyclic units inferred by Mathison (1987), the rock densities, and the modal compositions. Unit 3, the thickest unit in the sequence, is noteworthy by being different from the other cyclic units. It appears to compromise two incomplete cyclic units in which the sequences are anorthosite–troctolite (unit 3A) and leucotroctolite–troctolite–olivine gabbro (unit 3B). In the leucotroctolite is the best developed zone of small-scale rhythmic banding within the macrolayers of the intrusion. Unit 4 is also very different in that there is a 5-m-thick zone with about 7% olivine occurring near the middle of the anorthosite at the base of the unit's sequence, so that the lower 30 m of unit 4 could be an incomplete or interrupted cyclic unit, with the sequence anorthosite–troctolitic–anorthosite followed by the typical cyclic sequence from anorthosite through to oxide gabbro.

## Previous Radioisotopic Dating

The currently accepted conventional age of the Somerset Dam layered gabbro intrusion is based on two sets of K-Ar determinations reported by Webb & McDougall (1967). They made two measurements on hornblende from a hornblende gabbro near the top of the intrusion, and two measurements on plagioclase from an olivine gabbro near the bottom of the intrusion. Murphy, Trezise, Hutton, Cranfield, & Whittaker (1979) and Murphy, Trezise, Hutton, & Cranfield (1987) recalculated the resultant K-Ar dates using the IUGS constants of Dalrymple (1979). Thus the hornblende yielded revised "ages" of 218 and 220 Ma, and the plagioclase yielded revised K-Ar "ages" of 212 and 213 Ma. Of course, it would be expected on the

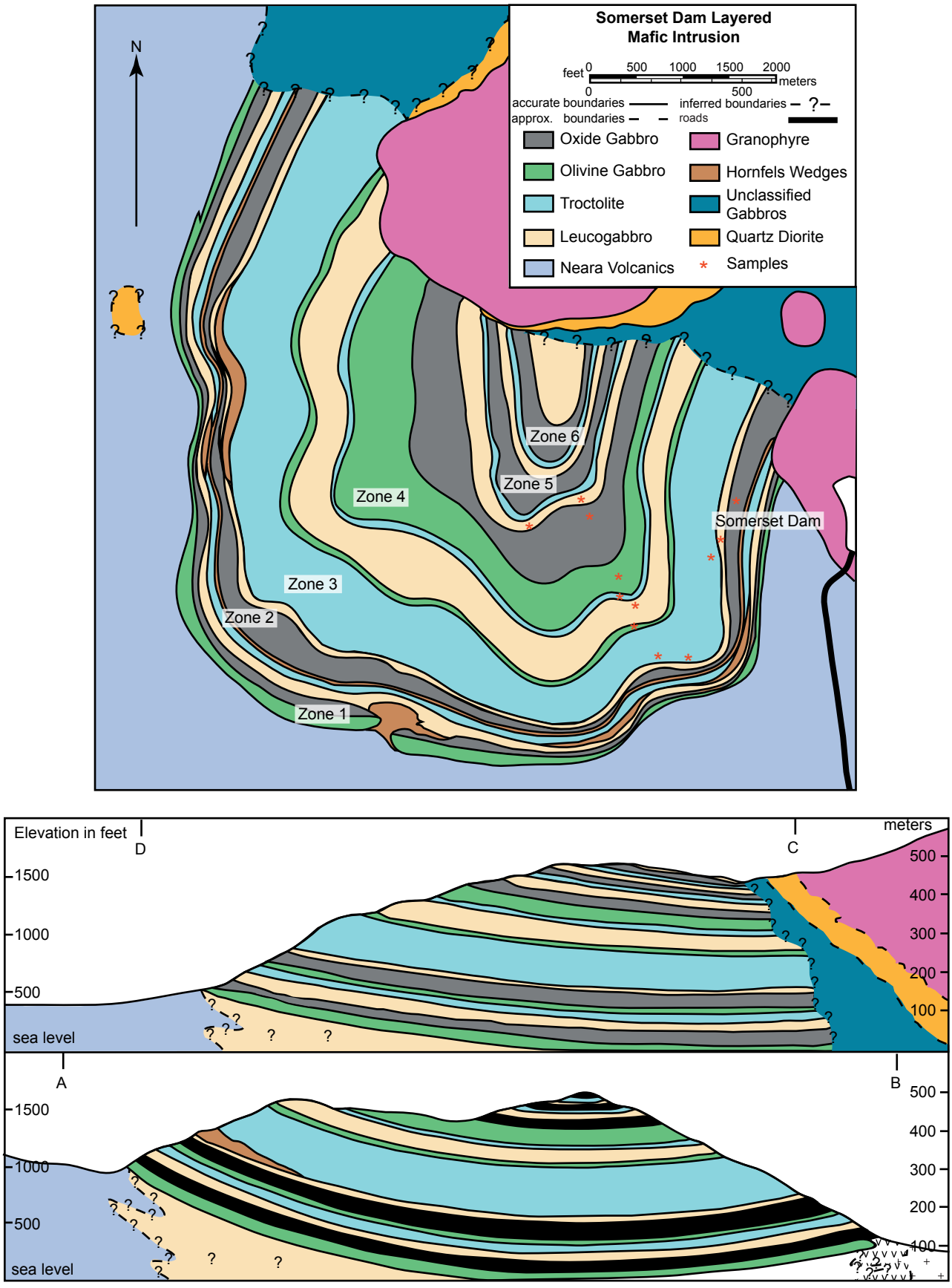


**Figure 2.** Geological map (top) and cross-sections (bottom) of the Somerset Dam layered mafic intrusion (after Mathison, 1967).

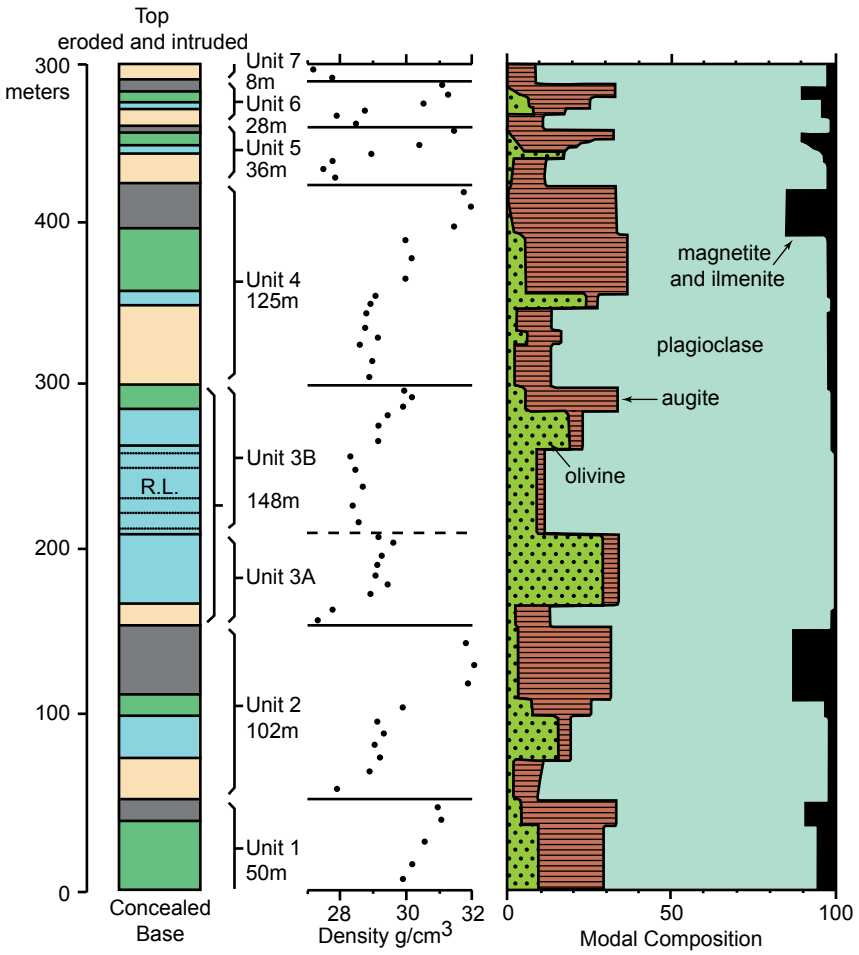


**Figure 3.** Stratigraphic column for the Somerset Dam Layered Mafic Intrusion (after Mathison, 1987) showing inferred cyclic units, rock densities, and modal compositions (blank = leucogabbro; dotted = troctolite; dashed = olivine gabbro; black = oxide gabbro; R.L. = best developed zone of rhythmic layering).

assumption of the sequential crystallization of the layering within the intrusion that the dates from the olivine gabbro near the bottom of the intrusion should be older than the dates from the hornblende gabbro near the top, but it is reasonable to attribute these differences in the age determinations to the "within error" of the technique. Taking these results as a group yields an "averaged age" of 216±4Ma.

Walker (1998) separated hornblende grains from the troctolite in cyclic unit 2 and the olivine gabbro in cyclic unit 4, and used the argon laser incremental heating technique to make $^{40}Ar/^{39}Ar$ age determinations. Only the hornblende grains from the olivine gabbro yielded a calculated "apparent age" of 221.5±0.9Ma. Determinations were also made on K-feldspar, muscovite, and biotite grains of alkali feldspar granite (granophyre) and quartz monzodiorite units which he interpreted as being related to the layered intrusion (Figure 2), and together with the hornblende result, a "pooled apparent age" of 224.2±4.8Ma was calculated for the entire Somerset Dam igneous complex. Similarly, Walker (1998) undertook Rb-Sr age determinations on whole-rock samples of all four rock types in the layered intrusion plus the nearby peripherally-related igneous units, as well as mineral determinations for an olivine gabbro and the peripheral granite (granophyre). An isochron fitted to all these data using all the whole-rock samples and all the mineral separates yielded an "acceptable" Rb-Sr isochron "age" for the whole Somerset Dam igneous complex of 225.3±2.3Ma, which thus agreed remarkably well with the pooled apparent Ar-Ar age.

## Sample Collection

The field work and collection of samples was undertaken in June 1998 and November 1999. Access to suitable outcrops was provided by a farm road that starts at the village of Somerset Dam, from the highway into the village and the dam itself, which is a spur from the Brisbane Valley Highway just north of the town of Esk. The farm access road climbs the hillside just to the west of the village and the dam, which is the hill containing the layered gabbro intrusion. Thus the road progressively climbs up through the different macrolayers of the intrusion, with suitable outcrops in roadcuts and on the hillside either side of the road. During the June 1998 field trip, twelve 2–3kg samples were collected along this road traverse through the intrusion, commencing with a sample of the oxide gabbro at the top of cyclic unit 2 (Mathison, 1987), with samples of all the successive macrolayers for units 3 and 4, to two samples of the anorthosite macrolayer at the base of unit 5. The locations of these samples are marked on Figure 2. During the November 1999 field trip a series of six 3–4kg closely-spaced samples were collected from the oxide gabbro macrolayer at the top of cyclic unit 2. The purpose of the close-spaced sampling was to investigate mineralogical and geochemical variations within a macrolayer, and particularly to choose one suitable sample for separation into its mineral constituents for radioisotopic dating of them in order to produce mineral isochrons, work still in progress. The locations of these samples are also marked on Figure 2.

## Laboratory Work

All samples were sent first for sectioning—one thin section from each sample for petrographic analysis. Four of the six closely-spaced samples from the oxide gabbro macrolayer at the top of cyclic unit 2 were then selected for analysis, along with the 11 samples from the overlying macrolayers of units 3 and 4, and the anorthosite at the base of unit 5. Approximately 100 g of each of these samples was dispatched to the AMDEL Laboratory in Adelaide, South Australia, for whole-rock major, trace and rare earth element analyses. A second representative set of pieces (50–100 g) of each of these samples was then sent to the K-Ar dating laboratory at Activation Laboratories in Ancaster, Ontario, Canada, for whole-rock K-Ar dating. A third representative set of pieces (50–100 g) of each of these samples was also sent to the PRISE Laboratory in the Research School of Earth Sciences at the Australian National University in Canberra, Australia, for whole-rock Rb-Sr, Sm-Nd, and Pb-Pb radioisotopic dating.

At the AMDEL Laboratory each sample was crushed and pulverized. Whole-rock analyses were undertaken by total fusion of each powdered sample and then digesting them before ICP-OES (inductively coupled plasma—optical emission spectrometry) for major and minor elements, and ICP-MS (inductively coupled plasma—mass spectrometry) for trace and rare earth elements. Fe was analyzed for among the major elements by ICP-OES as $Fe_2O_3$ and reported accordingly, but separate analyses for Fe as FeO were also undertaken via wet chemistry methods that were also able to record the loss on ignition, primarily representing $H_2O$ or any carbonate (given off as $CO_2$) in the samples. The detection limit for all major element oxides was 0.01%. For minor and trace elements the detection limits varied between 0.5 and 20 ppm, and for rare earth elements between 0.5 and 1 ppm.

At Activation Laboratories the K-Ar analyses were performed under the direction of the K-Ar Laboratory manager, Dr. Yakov Kapusta. No specific location or expected age information was supplied to the laboratory, but a description of the samples was given so that the laboratory staff knew the types of samples they were dealing with and could ensure their procedures were conducted appropriately. After crushing of the whole-rock samples and pulverizing them, the concentrations of K (weight %) were measured by the ICP technique. The $^{40}K$ concentrations (ppm) were then calculated from the terrestrial isotopic abundance using these measured concentrations of K. The concentrations in ppm of $^{40}Ar^*$, the supposed radiogenic $^{40}Ar$, were derived using the conventional formula from isotope dilution measurements on a noble gas mass spectrometer by correcting for the presence of atmospheric argon whose isotopic composition is known (Dalrymple & Lanphere, 1969). The ratios $^{40}Ar^*$/total Ar and $^{40}Ar/^{36}Ar$ were also derived from the mass spectrometer measurements.

The Rb-Sr, Sm-Nd, and Pb-Pb isotopic analyses were undertaken at the PRISE Laboratory under the direction of Dr. Richard Armstrong. No specific location or expected age information was supplied to the laboratory, although samples were described as young gabbros so that the laboratory staff would optimize the sample preparation procedure in order to obtain the best analytical results. At the laboratory the sample pieces were crushed and pulverized before being dissolved in concentrated hydrofluoric acid, followed by the standard chemical separation procedures for each of these radioisotope systems. Once separated, the elements in each radioisotope system were loaded by standard procedures onto metal filaments to be used in the solid source thermal ionization mass spectrometer (TIMS), the state-of-the-art technology in use in this laboratory. Sr isotopes were measured using the mass fractionation correction $^{86}Sr/^{88}Sr=0.1194$, and the $^{87}Sr/^{86}Sr$ ratios reported are normalized to the NBS standard SRM 987 value of 0.710207. Nd isotopes were corrected for mass fractionation using $^{146}Nd/^{144}Nd=0.7219$ and are normalized to the present-day $^{143}Nd/^{144}Nd$ value of 0.51268 for BCR-1. Pb isotope ratios are normalized to NBS standard SRM 981 for mass fractionation.

## Petrography and Chemistry

Each cyclic unit commences at its base with a macrolayer of leucogabbro (plagioclase cumulate or anorthosite). Plagioclase (labradorite, 84% average modal composition [Mathison, 1967]) is the main cumulus phase in the leucogabbros, with very minor cumulus olivine (trace) and sometimes traces of cumulus magnetite. Intercumulus minerals (which crystallized subsequent to, and therefore in the remaining space between, the cumulus phases [Hall, 1998]) in order of decreasing abundance include augite (3%), brown hornblende (3%), ilmenite (2%), magnetite (1%), apatite (0.4%), and orthopyroxene (0.1%). The crystallization order is thus inferred to have been plagioclase first, then minor olivine (if present), augite, magnetite and ilmenite, rare orthopyroxene, brown hornblende, and finally apatite. The leucogabbros are consistently more altered than the other rock types, and the augite (invariably ophitic or poikilitic) is usually highly altered to felted aggregates of a low-Al actinolitic pale green amphibole ("uralite," 6% average modal composition), which is thus commonly the next most abundant mineral to plagioclase. The leucogabbros are mainly orthocumulates (Hall) as indicated by their overall texture, the proportion

of intercumulus minerals, the relatively abundant brown hornblende, the extensive normal zoning in plagioclase (15–20 mole% An [anorthite]), the generally higher content of incompatible elements such as K and P, and probably also by the extensive alteration that probably reflects a relatively high trapped fluid content upon crystallization (Mathison, 1987).

Cumulus phases in the troctolites (plagioclase-olivine cumulates) include plagioclase (labradorite, 75% average modal composition (Mathison, 1967), olivine (18%) and traces of Cr-magnetite, while the intercumulus minerals include mainly augite (3%), brown hornblende (0.5%), magnetite (0.4%) and ilmenite (0.6%), with trace amounts of orthopyroxene and apatite. The crystallization order is inferred to have been the same as for the leucogabbros, except that minor Cr-magnetite crystallized early, possibly after plagioclase. At least some of the plagioclase had to have crystallized before the olivine because olivine grains commonly contain small laths of plagioclase. The plagioclase laths are generally smaller and thinner than in the other rock types of the intrusion, and they are strongly laminated. Olivine grains are subhedral when enclosed in augite, but are partly interstitial with respect to plagioclase. Augite grains are always poikilitic or ophitic, and enclose numerous laths of plagioclase and a few grains of olivine. However, the modal proportion and texture of augite also varies, and the troctolite in unit 4 particularly has conspicuous augite oikocrysts (5–10 mm diameter). Nevertheless, the main variation in the troctolites is in the relative modal proportions of plagioclase and olivine (see Figure 3), those troctolites with >80% plagioclase being leucotroctolites. Some alteration of the augite has again resulted in aggregates of uralite, which can reach an average modal composition of 2% (Mathison, 1967).

In the olivine gabbros (plagioclase-augite-olivine cumulates) cumulus augite (20% average modal composition (Mathison, 1967) joins the cumulus assemblage of plagioclase (labradorite, average 68%) and olivine (average 6%) of the troctolites, and the intercumulus minerals are mainly brown hornblende (2%), magnetite (1%), ilmenite (1%), very minor orthopyroxene (average 0.2%) occurring exclusively as partial reaction rings on some olivine grains, and trace apatite. The crystallization order was probably similar to that for the leucogabbros. The augite is subhedral and twinned, and never surrounds olivine. Again, it can be altered to uralite, which sometimes averages 1.5%. The brown hornblende is often ophitic and may be present in amounts up to 5% by volume. Transitions between olivine gabbros and oxide gabbros are observed in the upper cyclic units.

Cumulus phases in the oxide gabbros (plagioclase-augite-magnetite-ilmenite cumulates) are mainly plagioclase (labradorite, 55% average modal composition [Mathison, 1964]) and augite (average 28%) with 0–3% olivine, some magnetite (average 7%) and ilmenite (average 6%). At least some of the magnetite is cumulus (subhedral octahedral), but extensive intercumulus overgrowth has occurred so that most Fe-Ti oxide grain boundaries are interstitial to plagioclase and augite. The augite is frequently twinned, and occurs as well-defined subhedral prisms. Although alteration of the oxide gabbros is minimal, there are still some traces of uralite. Some brown hornblende is again present (up to an average of 1.5%), and other intercumulus minerals are rare, while orthopyroxene is completely absent. The oxide gabbros have the most adcumulate character, that is, during magmatic crystallization the interstitial liquid had been displaced by outgrowth from the cumulus crystals so that the latter are interlocking (Hall, 1998). The oxide gabbros are also the most fractionated compositions of the four main rock types in a typical cyclic unit. Though originally termed "ferrigabbros" by Mathison (1967), because the total iron content is similar to that of some of the ferrogabbros in the Skaergaard layered mafic intrusion in east Greenland, in these Somerset Dam gabbros the $Fe^{3+}/Fe^{2+}$ is high (>0.7) due to the abundant magnetite, so Mathison (1987) referred to them as oxide gabbros.

The whole-rock major element oxide and selected trace and rare earth element analytical results from the 15 samples selected for this study are listed in Table 1. The distribution of the major element oxides between the four different rock types in the macrolayers of each cyclic unit follows the pattern in the average whole-rock major element oxide compositions for these rocks already reported by Mathison (1967, 1987). The oxide gabbros have the lowest $SiO_2$ and highest $Fe_2O_3$ contents, and the anorthosites (leucogabbros) have the highest $SiO_2$ and lowest $Fe_2O_3$ contents. The $Al_2O_3$ content is highest in anorthosite at the base of each cyclic unit and decreases upwards through troctolite and olivine gabbro to the lowest content in the oxide gabbro, which parallels the decreasing plagioclase content (Mathison, 1967) (see Figure 3). Mathison (1987) found that the compositional changes with increasing height and increasing fractionation in a typical cyclic unit were clearly evident from the major element oxide data, such as that in Table 1, and generally involve increases in total iron (both $Fe^{2+}$ and $Fe^{3+}$), the $Fe^{3+}/Fe^{2+}$ratio, $TiO_2$ and MnO, and decreases in $Al_2O_3$, $SiO_2$, $Na_2O$, and $K_2O$.

The selected trace and rare earth element data in Table 1 are also similar to the comparable data obtained by Mathison (1987) and Walker (1998). In summary, Cr, Ni, V, and Cu show the greatest variation both within a cyclic unit and throughout the

**Table 1.** Whole-rock major element oxide and selected trace element analyses of 15 samples from the Somerset Dam layered mafic intrusion, near Brisbane, Australia. (Analyst: AMDEL, Australia; April, 2000).

| Sample | SDI-2A1 | SDI-2A3 | SDI-2A4 | SDI-2A6 | SDI-2B | SDI-3A | SDI-3B | SDI-3C | SDI-3D | SDI-3E | SDI-4A | SDI-4B | SDI-4C | SDI-4D | SDI-4E |
|---|---|---|---|---|---|---|---|---|---|---|---|---|---|---|---|
| Rock Type | Oxide Gabbro | Oxide Gabbro | Oxide Gabbro | Oxide Gabbro | Anorthosite | Troctolite | Troctolite | Troctolite | Olivine Gabbro | Anorthosite | Troctolite | Olivine Gabbro | Oxide Gabbro | Anorthosite | Anorthosite |
| Cyclic Unit | 2 | 2 | 2 | 2 | 3 | 3 | 3 | 3 | 3 | 4 | 4 | 4 | 4 | 5 | 5 |
| $SiO_2$ (%) | 43.6 | 45.3 | 44.2 | 39.9 | 47.5 | 48.1 | 45.9 | 46.8 | 50.9 | 49.1 | 48.4 | 47.2 | 43.8 | 50.7 | 50.9 |
| $TiO_2$ (%) | 4.75 | 3.97 | 3.91 | 5.21 | 0.30 | 0.58 | 0.41 | 0.33 | 0.49 | 0.50 | 0.52 | 1.27 | 4.85 | 1.13 | 0.88 |
| $Al_2O_3$ (%) | 14.6 | 17.1 | 17.2 | 17.2 | 25.5 | 21.3 | 18.1 | 24.6 | 20.1 | 24.1 | 20.7 | 20.2 | 15.9 | 25.5 | 24.8 |
| $Fe_2O_3$ (%) | 15.4 | 12.6 | 12.8 | 19.2 | 4.70 | 6.76 | 9.00 | 5.08 | 4.59 | 4.77 | 7.50 | 10.4 | 15.1 | 5.63 | 5.49 |
| MgO (%) | 5.98 | 5.57 | 5.85 | 7.77 | 6.54 | 8.65 | 14.0 | 6.97 | 6.46 | 4.67 | 8.72 | 6.19 | 5.56 | 2.07 | 2.62 |
| MnO (%) | 0.19 | 0.14 | 0.13 | 0.18 | 0.07 | 0.10 | 0.14 | 0.08 | 0.08 | 0.08 | 0.12 | 0.11 | 0.15 | 0.06 | 0.08 |
| CaO (%) | 11.5 | 10.5 | 10.9 | 6.64 | 12.3 | 10.3 | 9.84 | 11.9 | 13.2 | 12.4 | 10.4 | 10.9 | 11.8 | 10.3 | 10.2 |
| $Na_2O$ (%) | 2.55 | 3.17 | 3.19 | 2.79 | 2.30 | 2.85 | 1.91 | 2.27 | 3.04 | 2.99 | 2.77 | 3.03 | 2.39 | 3.92 | 4.02 |
| $K_2O$ (%) | 0.15 | 0.24 | 0.23 | 0.12 | 0.12 | 0.20 | 0.09 | 0.14 | 0.18 | 0.27 | 0.22 | 0.19 | 0.11 | 0.27 | 0.49 |
| $P_2O_5$ (%) | 0.23 | 0.30 | 1.20 | 0.04 | 0.06 | 0.11 | 0.04 | 0.06 | 0.04 | 0.15 | 0.07 | 0.05 | 0.01 | 0.06 | 0.08 |
| LoI (%) | 0.57 | 0.09 | 0.17 | 0.77 | 0.89 | 0.99 | 0.91 | 1.36 | 0.55 | 0.94 | 0.86 | 0.22 | 0.43 | 0.54 | 1.07 |
| TOTAL | 99.52 | 98.98 | 99.78 | 99.52 | 100.28 | 99.94 | 100.34 | 99.59 | 99.63 | 99.97 | 100.28 | 99.76 | 100.1 | 100.18 | 100.63 |
| Cr (ppm) | 70 | 70 | 60 | 20 | 90 | 100 | 200 | 120 | 550 | 200 | 380 | 140 | 40 | 40 | 70 |
| V (ppm) | 470 | 340 | 340 | 440 | 30 | 60 | 60 | 40 | 90 | 60 | 70 | 350 | 550 | 140 | 110 |
| Ni (ppm) | 26 | 5 | 5 | 7 | 92 | 115 | 230 | 91 | 36 | 39 | 81 | 49 | 7 | 4 | 3 |
| Co (ppm) | 40 | 40 | 40 | 60 | 30 | 40 | 60 | 30 | 20 | 20 | 40 | 60 | 50 | 20 | 20 |
| Cu (ppm) | 90 | 84 | 250 | <2 | 12 | 32 | 33 | 13 | 38 | 20 | 45 | 210 | 60 | 13 | 4 |
| Zn (ppm) | 83 | 59 | 59 | 94 | 34 | 46 | 63 | 55 | 33 | 45 | 55 | 60 | 79 | 42 | 74 |
| Rb (ppm) | 4.5 | 4.5 | 3.5 | 1.5 | 2.5 | 3.5 | 1.5 | 2.5 | 3.5 | 5.0 | 4.0 | 3.5 | 1.5 | 5.0 | 15.5 |
| Sr (ppm) | 450 | 550 | 500 | 550 | 600 | 450 | 400 | 550 | 470 | 550 | 490 | 500 | 410 | 700 | 700 |
| Y (ppm) | 16 | 11 | 16 | 2 | 4 | 7 | 6 | 5 | 9 | 10 | 10 | 6 | 9 | 4 | 7 |
| Zr (ppm) | 90 | 60 | 50 | 40 | 30 | 40 | 30 | 30 | 30 | 40 | 50 | 40 | 40 | 40 | 50 |
| Ba (ppm) | 50 | 60 | 60 | 40 | 45 | 45 | 30 | 40 | 50 | 65 | 60 | 55 | 35 | 75 | 100 |
| Pb (ppm) | 25 | 20 | 15 | 30 | <5 | <5 | <5 | <5 | <5 | 10 | <5 | <5 | 25 | 5 | 5 |
| Th (ppm) | 33.5 | 20.5 | 18.5 | 17.5 | 9.5 | 11.0 | 12.0 | 9.5 | 10.0 | 9.5 | 11.0 | 11.5 | 14.0 | 8.0 | 8.5 |
| U (ppm) | 1.5 | 0.5 | <0.5 | <0.5 | <0.5 | <0.5 | <0.5 | <0.5 | <0.5 | <0.5 | <0.5 | <0.5 | <0.5 | <0.5 | <0.5 |
| La (ppm) | 11 | 9 | 13 | 6 | 7 | 9 | 6 | 7 | 7 | 9 | 8 | 7 | 6 | 8 | 10 |
| Ce (ppm) | 12 | 10 | 16 | 3 | 5 | 9 | 6 | 7 | 9 | 12 | 10 | 8 | 6 | 8 | 10 |
| Nd (ppm) | 13.5 | 9.0 | 16.0 | 2.0 | 4.5 | 6.5 | 4.0 | 4.0 | 5.5 | 7.5 | 7.0 | 4.5 | 4.5 | 4.5 | 6.0 |
| Sm (ppm) | 3.5 | 2.5 | 4.0 | <0.5 | 1.0 | 1.5 | 1.0 | 1.0 | 1.5 | 2.0 | 2.0 | 1.0 | 1.5 | 1.0 | 1.5 |

**Table 2.** Whole-rock K-Ar data for the Somerset Dam layered mafic intrusion, near Brisbane, Australia. (Analyst: Dr. Y. Kapusta, Activation Laboratories, Ancaster, Canada; April, 2001). These data yield 15 point isochron ages of 174±8 Ma (K-Ar) and 181±23 Ma ($^{40}K/^{36}Ar$—$^{40}Ar/^{36}Ar$).

| Sample Code | Rock Type | $K_2O$ (wt%) | $^{40}K$ (ppm) | $^{40}Ar^*$ (ppm) | Total $^{40}Ar$ (ppm) | $\frac{^{40}Ar}{^{36}Ar}$ | $^{36}Ar$ (ppm) | $\frac{^{40}K}{^{36}Ar}$ | Model Age (Ma) | Uncertainty (Ma) (1 sigma) |
|---|---|---|---|---|---|---|---|---|---|---|
| SDI-4E | Leuco Gabbro | 0.498 | 0.493 | 0.005445 | 0.007467 | 405.96 | 0.0000183 | 26939.9 | 184.2 | ±7 |
| SDI-4D | Leuco Gabbro | 0.302 | 0.299 | 0.003516 | 0.004254 | 359.54 | 0.0000118 | 25338.9 | 195.1 | ±8 |
| SDI-4C | Oxide Gabbro | 0.166 | 0.165 | 0.001804 | 0.002040 | 334.72 | 0.0000060 | 27500.0 | 182.7 | ±9 |
| SDI-4B | Olivine Gabbro | 0.223 | 0.221 | 0.002676 | 0.002945 | 325.73 | 0.0000090 | 24555.6 | 201.1 | ±8 |
| SDI-4A | Troctolite | 0.223 | 0.221 | 0.002398 | 0.002657 | 328.03 | 0.0000080 | 27625.0 | 181.3 | ±8 |
| SDI-3E | Leuco Gabbro | 0.224 | 0.222 | 0.002749 | 0.003588 | 386.34 | 0.0000092 | 24130.4 | 205.3 | ±8 |
| SDI-3D | Olivine Gabbro | 0.212 | 0.210 | 0.002692 | 0.003818 | 419.73 | 0.0000090 | 23333.3 | 211.9 | ±8 |
| SDI-3C | Troctolite | 0.140 | 0.138 | 0.001870 | 0.002397 | 379.43 | 0.0000063 | 21904.8 | 222.7 | ±7 |
| SDI-3B | Troctolite | 0.100 | 0.099 | 0.001532 | 0.001932 | 373.25 | 0.0000051 | 19411.8 | 252.8 | ±9 |
| SDI-3A | Troctolite | 0.198 | 0.231 | 0.002459 | 0.003134 | 377.34 | 0.0000083 | 27831.3 | 208.2 | ±9 |
| SDI-2B | Leuco Gabbro | 0.110 | 0.109 | 0.001590 | 0.001925 | 358.46 | 0.0000053 | 20566.0 | 240.3 | ±8 |
| SDI-2A6 | Oxide Gabbro | 0.100 | 0.009 | 0.001444 | 0.001851 | 379.55 | 0.0000048 | 20625.0 | 239.4 | ±9 |
| SDI-2A4 | Oxide Gabbro | 0.513 | 0.508 | 0.005953 | 0.009920 | 492.15 | 0.0000201 | 25273.6 | 194.7 | ±8 |
| SDI-2A3 | Oxide Gabbro | 0.251 | 0.248 | 0.002896 | 0.004060 | 415.04 | 0.0000097 | 25567.0 | 193.9 | ±7 |
| SDI-2A1 | Oxide Gabbro | 0.205 | 0.203 | 0.002250 | 0.003125 | 411.10 | 0.0000076 | 26710.5 | 184.9 | ±9 |

intrusion's stratigraphic succession. Furthermore, as expected, the pattern of variations in each cyclic unit of the major and trace elements parallels the changes in mineralogy. Thus the $P_2O_5$ content parallels the presence of accessory apatite, Sr parallels the abundance of plagioclase, and rare earth elements such as La, Ce, and Nd are often slightly more concentrated in the oxide gabbros. Mathison (1967, 1975, 1987) also analyzed the compositions of the major minerals (plagioclase, olivine, augite, orthopyroxene, brown hornblende, magnetite, ilmenite, and biotite) and plotted the compositional variations through each cyclic unit for the entire exposed stratigraphic sequence of the intrusion. He found that the most sensitive parameters for defining the cryptic compositional trends in the minerals are An in plagioclase, Fo and Ni in olivine, and Cr in magnetite and augite.

## Radioisotopic Dating Results

The K-Ar analytical data and K-Ar model "ages" for all 15 samples in this study are listed in Table 2. These model ages are calculated using the standard equation of Dalrymple & Lanphere (1969) utilizing the ratio of the abundances of $^{40}$Ar* (the radiogenic $^{40}$Ar) to $^{40}$K listed in Table 2. The model age method assumes no radiogenic $^{40}$Ar was present when the basaltic magma was intruded to form each cyclic unit, and as it differentiated to form the layered gabbros while cooling. The model ages range from 181.3±8Ma (one-sigma error) to 252.8±9Ma, with the mean "age" being 206.6Ma (+46.2Ma, 25.3Ma, n=15). The wide variation in these model ages is not able to be explained readily, because they do not form a predictable sequence of decreasing age with the formation of each cyclic unit in an ascending order from bottom to top of the intrusion. Indeed, there is no recognizable pattern, except that many of the model "ages" are discordant from one another. The mean model ages for the cyclic units sampled are 203.2Ma (n=4) for cyclic unit 2, 227.2Ma (n=5) for cyclic unit 3, 192.6Ma (n=4) for cyclic unit 4, and 189.7Ma (n=2) for cyclic unit 5. Whereas there is an apparent younging trend upwards from cyclic unit 3 to cyclic units 4 and 5, cyclic unit 2, which should be the oldest of those sampled yields a mean model "age" younger than the overlying cyclic unit 3. Furthermore, where in cyclic units 3 and 4 the sequence of macrolayers has been sampled and analyzed, these macrolayers should all be the same age, because they differentiated and fractionated from the same pulse of intruded basaltic magma in each case, but the model "ages" obtained are discordant. Even where three troctolite samples were collected in ascending order within that macrolayer within cyclic unit 3, each of those troctolite samples yielded strongly discordant model ages. Similarly, samples SDI-2A4 and SDI-2A6, stratigraphically only several meters apart in the same oxide gabbro macrolayer in cyclic unit 2, yield strongly discordant model ages of 194.7±8Ma and 239.4±9Ma respectively.

Figure 4 is the $^{40}$K versus $^{40}$Ar* diagram in which all 15 samples from the Somerset Dam layered mafic intrusion have been plotted. The plotted error bars for each data point are the two-sigma uncertainties, but there is still a very strong linear trend apparent in the data, and this has been plotted as an isochron using the Isoplot program of Ludwig (2001) that utilizes the least-squares linear regression method of York (1969). All 15 samples were included in the regression calculation and produced an excellent fit. The isochron "age" calculated from the slope of the line is 174±8Ma (two-sigma error). The two-sigma uncertainty in this isochron age is very small because the two-sigma uncertainties assigned to each of the data points are

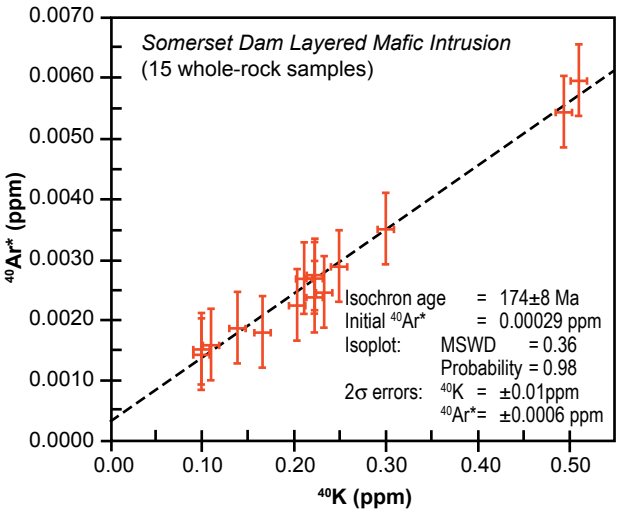


**Figure 4.** $^{40}$K versus $^{40}$Ar* in the Somerset Dam layered mafic intrusion, all 15 samples being used in the isochron and age calculations. The bars represent the two-sigma uncertainties.

also very small. The excellent fit of this isochron line to the data is highlighted by the very low MSWD (mean square weighted deviates—a measure of the ratio of the observed scatter of the data points from the best-fit line to the expected scatter from the assigned errors and error correlations) and the very high probability (0.98). The initial $^{40}$Ar* is 0.00029ppm, which is a very small quantity of excess radiogenic $^{40}$Ar in violation of the assumption of zero $^{40}$Ar* in the model age technique. This K-Ar isochron "age" is significantly discordant with the three sets of published K-Ar determinations on hornblende and plagioclase of Webb & McDougall (1967), recalculated by Murphy et al (1976; 1987) using the IUGS constants of Dalrymple (1979), of 218 and 220Ma, and 212 and 213Ma respectively, which yield an "averaged age" of 216±4Ma. Similarly, this 15-point K-Ar isochron "age" of 174±8Ma is strongly discordant with the "pooled apparent age" of 224.2±4.8Ma based on $^{40}$Ar/$^{39}$Ar determinations on three K-feldspar, four muscovite, one hornblende and four biotite grains by Walker (1998).

The whole-rock Rb-Sr, Sm-Nd, and Pb-Pb radioisotopic data for all 15 samples from the intrusion are listed in Table 3. As anticipated, the radioisotopic ratios in these 15 gabbro samples show little variation in all three radioisotope systems. This is because of the similar mineralogy in these gabbros, and in spite of the modal variations in these minerals between the different macrolayers. Even the significantly lower plagioclase and higher magnetite and ilmenite contents in the oxide gabbros compared to the leucogabbros (anorthosites) makes little difference in the variations in the respective radioisotopic ratios.

Figure 5 shows $^{87}$Rb/$^{86}$Sr plotted against $^{87}$Sr/$^{86}$Sr for the layered mafic intrusion, based on the data in Table 3. The error bars again represent the two-

**Table 3**. Whole-rock Rb-Sr, Sm-Nd, Pb-Pb radioisotope data for the Somerset Dam layered mafic intrusion, near Brisbane, Australia. (Analyst: Dr R.A. Armstrong, PRISE, Australian National University, Canberra; March-July 2002).

| Sample | Rock Type | Cyclical Unit | Rb (ppm) | Sr (ppm) | $^{87}Rb/^{86}Sr$ | $^{87}Sr/^{86}Sr$ | Sm (ppm) | Nd (ppm) | $^{147}Sm/^{144}Nd$ | $^{143}Nd/^{144}Nd$ | $\varepsilon_{Nd}$ ($t_o$) | $T_{DM}$ (Ma) | $^{206}Pb/^{204}Pb$ | $^{207}Pb/^{204}Pb$ | $^{208}Pb/^{204}Pb$ |
|---|---|---|---|---|---|---|---|---|---|---|---|---|---|---|---|
| SDI-2A1 | Oxide gabbro | 2 | 1.92 | 503.89 | 0.0110 | 0.702929 | 2.985 | 10.150 | 0.17782 | 0.512989 | +6.03 | 686.5 | 18.660 | 15.589 | 38.529 |
| SDI-2A3 | Oxide gabbro | 2 | 2.71 | 560.94 | 0.0140 | 0.702944 | 2.632 | 7.753 | 0.20531 | 0.512990 | +6.05 | 2923.0 | 18.721 | 15.702 | 38.748 |
| SDI-2A4 | Oxide gabbro | 2 | 7.83 | 596.40 | 0.0380 | 0.703103 | 4.878 | 18.673 | 0.15797 | 0.512956 | +5.38 | 532.3 | 18.518 | 15.600 | 38.396 |
| SDI-2A6 | Oxide gabbro | 2 | 1.38 | 622.82 | 0.0064 | 0.702916 | 0.366 | 1.679 | 0.13178 | 0.512913 | +4.54 | 442.3 | 18.458 | 15.572 | 38.310 |
| SDI-2B | Anorthosite | 3 | 2.05 | 710.08 | 0.0083 | 0.702827 | 0.821 | 3.571 | 0.13908 | 0.512939 | +5.05 | 432.3 | 18.520 | 15.578 | 38.382 |
| SDI-3A | Troctolite | 3 | 3.77 | 534.20 | 0.0204 | 0.702740 | 1.301 | 5.400 | 0.14568 | 0.512923 | +4.74 | 510.2 | 18.538 | 15.578 | 38.422 |
| SDI-3B | Troctolite | 3 | 1.26 | 498.63 | 0.0073 | 0.702777 | 0.724 | 3.265 | 0.13411 | 0.512922 | +4.72 | 437.9 | 18.510 | 15.590 | 38.389 |
| SDI-3C | Troctolite | 3 | 2.19 | 604.88 | 0.015 | 0.702852 | 0.823 | 3.718 | 0.13394 | 0.512906 | +4.41 | 467.6 | 18.532 | 15.610 | 38.443 |
| SDI-3D | Olivine gabbro | 3 | 2.85 | 644.68 | 0.0128 | 0.702919 | 1.643 | 5.584 | 0.17789 | 0.512986 | +5.97 | 700.6 | 18.632 | 15.598 | 38.550 |
| SDI-3E | Anorthosite | 4 | 3.23 | 631.03 | 0.0148 | 0.702909 | 1.374 | 5.579 | 0.14893 | 0.512931 | +4.90 | 516.9 | 18.393 | 15.570 | 38.252 |
| SDI-4A | Troctolite | 4 | 4.38 | 615.34 | 0.0206 | 0.702957 | 1.170 | 5.266 | 0.13438 | 0.512902 | +4.33 | 477.9 | 18.739 | 15.625 | 38.690 |
| SDI-4B | Olivine gabbro | 4 | 3.59 | 625.00 | 0.0166 | 0.702925 | 1.130 | 4.148 | 0.16474 | 0.512951 | +5.29 | 657.2 | 18.551 | 15.601 | 38.455 |
| SDI-4C | Oxide gabbro | 4 | 1.33 | 450.68 | 0.0085 | 0.702979 | 1.427 | 4.394 | 0.19644 | 0.512986 | +5.97 | 1454.4 | 18.613 | 15.605 | 38.513 |
| SDI-4D | Anorthosite | 5 | 5.06 | 820.25 | 0.0178 | 0.703041 | 1.144 | 4.867 | 0.14215 | 0.512906 | +4.41 | 521.3 | 18.861 | 15.604 | 38.611 |
| SDI-4E | Anorthosite | 5 | 16.40 | 786.68 | 0.0603 | 0.703138 | 1.414 | 6.242 | 0.13694 | 0.512909 | +4.47 | 479.9 | 18.547 | 15.562 | 38.395 |

Notes: (1) Measured, present-day $^{87}Sr/^{86}Sr$ ratios (±2σ) are normalized to $^{86}Sr/^{88}Sr = 0.1194$

(2) The $^{87}Sr/^{86}Sr$ ratios are reported relative to a value of 0.710207±26 (±2σ) for the NBS standard SRM987 run with these samples.

(3) Measured, present-day $^{143}Nd/^{144}Nd$ ratios (±2σ) are normalized to $^{146}Nd/^{144}Nd = 0.7219$

(4) $\varepsilon_{Nd}$ ($t_0$) refers to the present-day, calculated value relative to a depleted mantle value of 0.51268 for BCR-1

(5) Depleted mantle model ages ($T_{DM}$) calculated using present-day depleted mantle values of $^{143}Nd/^{144}Nd = 0.51315$ and $^{147}Sm/^{144}Nd = 0.2136$

(6) $^{206}Pb/^{204}Pb$ ratios are normalized to NBS standard SRM981 for mass fractionation, while all other ratios are calculated by a double spiking routine.

sigma uncertainties in the data points, which were small in absolute terms but appear quite large with respect to the measured radioisotopic ratios, as can be seen in Figure 5. The regression analysis using the Isoplot program of Ludwig (2001) yielded a reasonable isochron fit to 14 of the 15 samples, with a reasonably low MSWD and a moderate probability. The troctolite sample SDI-3A is quite clearly an outlier. The resultant isochron "age" of 393±170Ma has a large two-sigma error, because of both the two-sigma uncertainties of the data points and the very narrow spread in the $^{87}Rb/^{86}Sr$ ratios of the data points. This 14-point whole-rock Rb-Sr isochron "age" appears to be significantly higher than the 12-point composite whole-rock (eight samples) and mineral (four minerals) Rb-Sr isochron "age" of 225.3±2.3Ma obtained by Walker (1998). Even though the two-sigma error envelope of the higher Rb-Sr isochron age obtained here includes the lower Rb-Sr isochron age of Walker and its two-sigma error envelope, the higher age does appear discordant in absolute terms with the younger age. The initial $^{87}Sr/^{86}Sr$ ratio obtained here is much higher than that obtained from the isochron fit of Walker, so if the anorthosite sample SDI-4E is also excluded from the regression analysis here, the resultant isochron line is significantly steepened with a slightly lower initial $^{87}Sr/^{86}Sr$ ratio, and thus yields an even higher isochron "age" of 572±310Ma (Figure 5) that is clearly discordant with the Walker Rb-Sr isochron age.

Figure 6 is the $^{147}Sm/^{144}Nd$ versus $^{143}Nd/^{144}Nd$ diagram on which all 15 data points for the Somerset Dam layered mafic intrusion in Table 3 have been plotted. The regression analysis on all 15 data points using the Isoplot program of Ludwig (2001) yielded

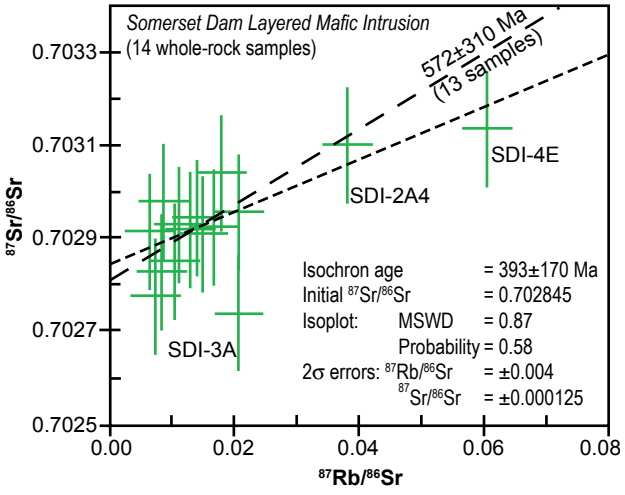


**Figure 5.** $^{87}Rb/^{86}Sr$ versus $^{87}Sr/^{86}Sr$ diagram for the Somerset Dam layered mafic intrusion. Only 14 of the 15 samples were used in the isochron and age calculations. The bars represent the two-sigma uncertainties.

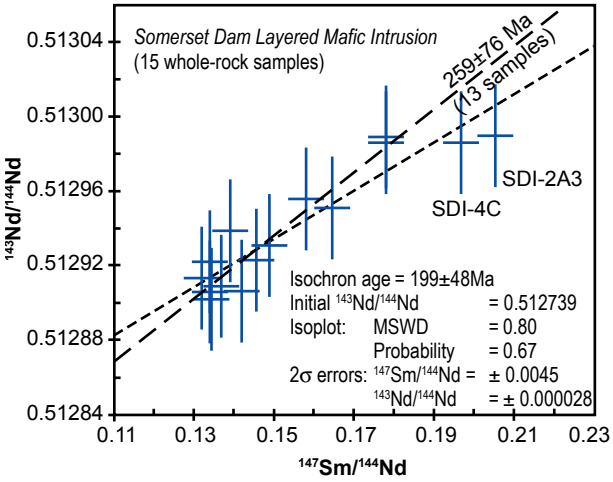


**Figure 6.** $^{147}Sm/^{144}Nd$ versus $^{143}Nd/^{144}Nd$ diagram for the Somerset Dam layered mafic intrusion, all 15 samples being used in the isochron and age calculations. The bars represent the two-sigma uncertainties.

a good-fitting isochron with a moderate probability and a low MSWD. The resultant isochron "age" of 199±48Ma has a moderate two-sigma error due to the narrow spread in the radioisotopic ratios, even though the two-sigma uncertainties for the individual data points are quite small in absolute terms. This all suggests that this is an acceptable Sm-Nd isochron "age" for this intrusion, which because of its moderate two-sigma error envelope would appear to be concordant with both the excellent 15-point whole-rock K-Ar isochron "age" of 174±8Ma obtained in this study, and the reasonable 12-point composite whole-rock and mineral Rb-Sr isochron "age" of 225.3±2.3Ma obtained by Walker (1998). Yet if the two oxide gabbro samples SDI-2A3 and SDI-4C are excluded from the regression analysis here, the slope of the resultant isochron line is significantly steeper, resulting in a much older 13-point Sm-Nd isochron "age" of 259±76Ma (Figure 6).

Figure 7 shows $^{206}Pb/^{204}Pb$ plotted against $^{207}Pb/^{204}Pb$ for the 15 whole-rock samples from the Somerset Dam layered mafic intrusion listed in Table 3. Only 13 of the 15 samples were used in the regression analysis (the oxide gabbro sample SDI-2A3 obviously being an outlier) and yielded an isochron fit with an "age" of 1425±1000Ma. The probability of this fit is moderate and the MSWD is reasonably low, while the two-sigma uncertainties in the data points (plotted as error ellipses in Figure 7) are reasonably small in absolute terms, yet the two-sigma error in the isochron "age" is unacceptably large because of the extremely narrow spread in the data points. Otherwise, it would be considered discordant with all other isochron "ages" obtained on this intrusion, apart perhaps from the Rb-Sr isochron "age" obtained in this study.

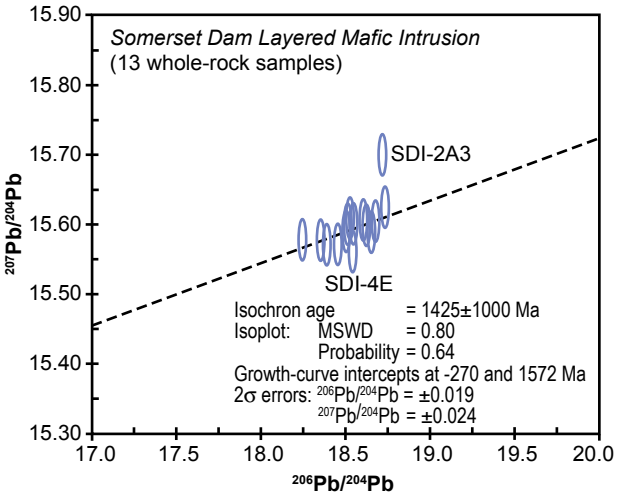


**Figure 7.** $^{206}Pb/^{204}Pb$ versus $^{207}Pb/^{204}Pb$ diagram for the Somerset Dam layered mafic intrusion. Only 13 of the 15 samples were used in the isochron and age calculations. The error ellipses represent the two-sigma uncertainties.

## Discussion

The Somerset Dam layered gabbro intrusion has been interpreted as a small sub-volcanic magma chamber located at some 3–5km depth, where each cyclic unit resulted from the entry of new magma into the chamber (Mathison, 1967, 1987). The question therefore arises as to whether it is legitimate to use these radioisotopic isochron techniques to date the intrusion, when each of these cyclic units in effect represents a distinct event in a time sequence of infillings of this sub-volcanic magma chamber. However, even in conventional timeframe these processes can be extremely rapid, conceivably occurring over hundreds of years or less (in conventional terms). Such time differences cannot be detected by these radioisotopic dating techniques, so the cyclic units in this intrusion are not only comagmatic and cogenetic, but are essentially coeval, which are necessary conditions for the application of these radioisotopic isochron techniques. In any case, this small sub-volcanic magma chamber has been interpreted as an open system with a connection to the surface, because a closed system would have resulted in a gradual increase in the degree of fractionation in successive cyclic units, which is observed in many large layered mafic intrusions such as the Skaergaard and Bushveld (McBirney & Noyes, 1979; Wager & Brown, 1968; Zingg, 1996), but which is not observed in this Somerset Dam layered mafic intrusion. As an open system this magma chamber would have had a connection to the surface through the overlying volcano, with space for successive magma renewals being made available by simultaneous venting periodically to the surface of a considerable volume of volcanic lavas. Unfortunately, the postulated vent system from this magma chamber is not now exposed, due to the top of the intrusion having been eroded away. Walker (1998) invoked a cyclic model involving a gradual increase and sudden release of pressure in the magma chamber that then explains a number of features of this layered gabbro intrusion, including the order of its layers, their inhomogeneity and lateral extent, the variations in grain sizes, the nature of the contact between each cyclic unit, and the similarity of the rock types in the macrolayers within the cyclic units. A gradual increase in pressure would have occurred after a blockage of the outlet conduit, followed by a sudden decrease when the blockage cleared with the next eruption. It is therefore obvious that this cyclic sequence responsible for macrolayering in this intrusion would not have required large amounts of time. Thus including samples of macrolayers from several cyclic units in regression analyses to obtain isochron "ages," as has been done in this study, is totally reasonable and permissible.

The isotope plots reveal extraordinary linearity within the $^{40}K$-$^{40}Ar$, $^{87}Rb$-$^{87}Sr$, $^{147}Sm$-$^{143}Nd$, and $^{207}Pb$-$^{206}Pb$-$^{204}Pb$ radioisotope systems. Each of the four radioisotope pairs produces a 15-point, whole-rock plot. The four data plots (Figures 4 through 7) contain 60 data points, with 57 points following the linear trends. It is both remarkable and significant that only three of the whole-rock data points plot slightly off the linear trends. There is no readily apparent explanation for this, except perhaps difficulties in the analytical procedures in obtaining precision and reproducibility because of the low levels in the samples of elements such as Pb, a comment made by Armstrong (personal communication) with respect to the Pb radioisotopic results plotted in Figure 7. The stray data point in Figure 5 is more problematic, the only other possible explanation being contamination from xenoliths known to occur within the intrusion (Mathison, 1967).

Giem (1997) has suggested the possibility that the remarkably linear radioisotope ratios in isochron plots were derived, not by radioactive decay, but by mixing of two compositionally-different magmas. Such a model has been discussed by Snelling, Austin, & Hoesch (2003) in the context of a granophyre magma (high K, Ar, Rb, Sm, Nd, and U) supposedly having been mixed with a diabase magma (lower K, Ar, Rb, Sm, Nd, and U) in different proportions to produce the Bass Rapids sill in Grand Canyon. Application of a similar mixing model to the Somerset Dam layered mafic intrusion would have to postulate that its macrolayering and cyclic units were produced by the mixing of two basaltic magmas with different compositions. These two magmas, and the various mixtures of them, would never have been in an isotopically homogeneous condition, so that the radioisotopes in them may then

have formed the mixing lines in Figures 4 through 7 without radioisotope decay within the rocks.

However, mineral isochron plots provide the data critical for testing this magma mixing model (Austin, 2000). Mineral phases within any single rock should be homogeneous, because the mixing model supposes rocks crystallized from large, locally mixed, batches of melt, and since crystallization radioisotope decay has been minor. Yet in the Bass Rapids sill Snelling et al (2003) found that the radioisotopes differed significantly between mineral phases within a diabase sample. Similarly, preliminary data obtained from the mineral phases of a gabbro sample from the Somerset Dam layered mafic intrusion show significant differences in their radioisotopic content. Thus, significant radioisotope decay, not mixing, is favored as the explanation for the extraordinary linearity in the isochron plots. Furthermore, the petrographic and geochemical data from the Somerset Dam intrusion, as from other layered mafic intrusions, argues strongly that instead "unmixing" has occurred as crystal fractionation and magmatic differentiation resulted in chemical and gravitational segregation from the initially homogeneous, molten condition of a single basaltic magma. Thus the best explanation is the exact opposite of the mixing model.

Thus the $^{40}K$-$^{40}Ar$, $^{87}Rb$-$^{87}Sr$, $^{147}Sm$-$^{143}Nd$, and $^{207}Pb$-$^{206}Pb$-$^{204}Pb$ radioisotopic data obtained in this study provide strong evidence that the cyclic units in the Somerset Dam layered gabbro intrusion were all intruded while in an isotopically mixed condition from the same homogeneous source. Indeed, primary evidence of the original homogeneous mixture of the Ar, Sr, Nd, and Pb isotopes both in the magma source and throughout all the sampled cyclic units of the layered intrusion is provided by the extraordinary linearity within the plots of the whole-rock radioisotopic data (Figures 4 through 7). This evidence is also consistent with other inferences about the rapid sequential intrusion and differentiation of the cyclic units of the intrusion derived from a chemically and isotopically homogeneous basaltic magma source. Even though some 30% of the parental basaltic magma may have crystallized in transit before entering the magma chamber (Walker, 1998), the subsequent mineralogical segregation to form the macrolayers within each cyclic unit was produced by crystal accumulation, fractional crystallization, and crystal differentiation as the residual magmatic fluid compositions changed (Hall, 1998). Therefore, at the time of intrusion each of the cyclic units and the macrolayers within them had the same Ar, Sr, Nd, and Pb isotopic ratios that were inherited from the homogeneous parental basaltic magma source. This has to be implicit in, and is conventionally by definition, the agreed initial condition of these coeval macrolayers and cyclic units in order for radioisotopic dating of the intrusion to be achievable.

However, the present parent-daughter radioisotopic ratios within the whole-rock samples from this intrusion do not produce a consistent picture of the age of the formation of this layered intrusion. Indeed, the four radioisotope systems yield whole-rock isochron "ages" that are discordant, so that it appears difficult to constrain the age of the intrusion. However, the K-Ar whole-rock isochron is the most tightly constrained with the best regression statistics, which thus suggests that 174±8Ma (two-sigma error) may be the true conventional age of the intrusion. On the other hand, this 15-point whole-rock K-Ar isochron age is strongly discordant with the 12-point combined whole-rock and mineral Rb-Sr isochron "age" of 225.3±2.3Ma (two-sigma error) obtained by Walker (1998), which in turn is discordant with the 14-point whole-rock Rb-Sr isochron age of 393±170Ma (two-sigma error) obtained in this study. However, Walker used four data points (spiked and unspiked whole-rock determinations, and spiked K-feldspar and muscovite determinations) from the one sample of alkali feldspar granite (granophyre) to dramatically improve the spread of the data when plotted on the $^{87}Rr/^{86}Sr$ versus $^{87}Sr/^{86}Sr$ diagram, based on the assumption that the granophyre is related to the layered gabbro intrusion as a late-stage differentiate from the same magma source. Yet the field relationships constrain the relative ages so that the granophyre was emplaced after the quartz diorite, which in turn was emplaced after the layered mafic intrusion (Mathison, 1967; Walker). Thus if the four granophyre data points are excluded from Walker's regression analysis because it is unclear exactly how the granophyre is related to the layered intrusion, except that it has a younger relative age, then his remaining eight data points do not define an Rb-Sr isochron and yield an age for the layered mafic intrusion. The scatter in his data is large and the spread of data is so small.

But what about the "pooled apparent age" of 224.2±4.8Ma (two-sigma error), based on $^{40}Ar/^{39}Ar$ determinations on three K-feldspar, four muscovite, one hornblende, and four biotite grains, that is supposed to be confirmation of this 12-point Rb-Sr isochron "age" of 225.3±2.3Ma (Walker, 1998)? Is this remarkably close agreement real or contrived? The reality is that the three K-feldspar and four muscovite grains analyzed came from the alkali feldspar granite (granophyre), while the four biotite grains came from a quartz monzodiorite that like the granophyre is younger relatively than the layered mafic intrusion, to which their relationship has not been clearly demonstrated. Thus only one hornblende grain from an olivine gabbro within the mafic layered

intrusion was used in the calculation of this "pooled apparent age," and that was only because it gave a similar age to the K-feldspar, muscovite and biotite grains from the granophyre and quartz monzodiorite (Walker). Indeed, a total of seven "integrated ages" were obtained on hornblende grains from just two samples from the layered mafic intrusion (the olivine gabbro and a troctolite), but these ages ranged from 55.2±6.7Ma to 221.5±0.9Ma (two-sigma error), which was clearly an unacceptable result. Thus neither the pooled Ar-Ar results nor the Rb-Sr isochron of Walker yield an acceptable concordant conventional age for only the Somerset Dam layered mafic intrusion. Therefore, it must be concluded that the 15-point whole-rock K-Ar isochron "age" of 174±8Ma (two-sigma error) obtained in this study is the most reliable conventional age determination for the Somerset Dam layered mafic intrusion, which implies that the conventional age reported in the literature should be revised upward from Late Triassic to Middle Jurassic.

This conventional age of 174±8Ma for the layered mafic intrusion therefore defines when the intrusion was isotopically homogeneous with respect to Ar. However, the 15-point Sm-Nd isochron plot (Figure 6) is strongly linear, giving the "age" for initial homogeneous Nd as 199±48Ma (two-sigma error), while the 14-point Rb-Sr isochron plot (Figure 5) is also strongly linear, yielding the "age" from initial homogeneous Sr as 393±170Ma (two-sigma error). Although the uncertainties associated with these Rb-Sr and Sm-Nd whole-rock isochrons are larger, their "ages" are somewhat discordant with the K-Ar isochron "age," particularly the Rb-Sr. How then could the same suite of whole rocks have Sr isotopes mix at 393±170Ma (Figure 5), but not have the Sr remixed within the whole rocks by the event that thoroughly mixed the Nd isotopes within the same whole rocks at 199±40Ma (Figure 6), while the production of $^{40}Ar^*$ from radioisotopic decay of $^{40}K$ only commenced at 174±8Ma (Figure 4), assuming no initial $^{40}A$ an event which presumably should have remixed both the Sr and Nd isotopes in the same whole rocks? While the excellent 15-point K-Ar whole-rock isochron "age" of 174±8Ma would seem most likely to be the true "age" of the initial isotopic mixing, no internally consistent "age" emerges from these radioisotopic data.

Austin (2000) has already documented four categories of discordance found in cogenetic suites of rocks, that thus test the assumptions of radioisotopic dating. The first of these categories is when two or more whole-rock isochron "ages" are discordant. The whole-rock radioisotopic data reported here from the Somerset Dam layered mafic intrusion thus call into question the assumptions of radioisotopic dating. However, as already argued, there is corroborative evidence that the layered gabbro intrusion initially had a homogeneous mixture of the same Ar, Sr, Nd, and Pb isotopic ratios as in its parental basaltic magma. Thus the assumption about initial conditions for the intrusion and these radioisotope systems must be valid, in spite of the isochron age discordances. Furthermore, the evidence for open-system behavior is limited to perhaps contamination of Sr in the Rb-Sr radioisotope system in one troctolite sample, so the closed-system assumption is not unreasonable. Therefore, as already suggested by Snelling et al (2003), the differences in these isochron ages could be due to changes in the decay rates of the different radioisotope systems at some time or times in the past, rather than being caused by errors in the determination of the radioisotopic decay "constants." According to Steiger & Jäger (1977), the U decay constants have been measured to four significant figures, so no significant errors would be expected to occur in the Pb-Pb systems. Steiger & Jäger also recommend the decay constant for $^{87}Rb$ of $1.42\times10^{-11}$ that is in wide use, but Begemann et al (2001) have recommended a figure of $1.406\pm0.008\times10^{-11}$. However, this small change in the decay constant would not close the discordance between the Rb-Sr and either the Pb-Pb or Sm-Nd systems. Furthermore, Begemann et al reported that the decay constant for $^{147}Sm$ has generally been agreed to have been determined to three significant figures ($6.54\times10^{-12}$).

Snelling et al. (2003) present data that indicate that the α-emitting radioisotopes ($^{238}U$, $^{235}U$, and $^{147}Sm$) yield older "ages" than the β-emitting radioisotopes ($^{87}Rb$ and $^{40}K$) when used to date the same geologic event. In other words, the discordances in their calculated isochron "ages" are due to the different parent radioisotopes decaying at different rates over the *same* time period since that geologic event. They found that their data are consistent with the possibility that α-decay was accelerated more than β-decay at some time or times in the past. While the same pattern of discordances between the α-emitting radioisotopes and the β-emitting radioisotopes is not as clearly evident in the radioisotopic whole-rock isochron dating of the formation of the Somerset Dam layered mafic intrusion, there is comparative consistency. Perhaps the inconsistencies are due to the youthfulness of the conventional age of the Somerset Dam layered mafic intrusion (Middle Jurassic) compared to the conventional age of the Bass Rapids diabase sill in Grand Canyon (Upper Precambrian). Additionally, the similarity in mineralogy of all the gabbros in the layered intrusion does not provide a large spread in the concentrations of the parent radioisotopes, so a shorter real-time period of accelerated decay would yield an even narrower spread in the values of the resultant daughter radioisotopes.

Furthermore, Snelling et al (2003) report that their data are also consistent with the possibility that the longer the half-life of the α- or β-emitting radioisotope the more its decay has been accelerated, relative to the other α- or β-emitting radioisotopes, at some time or times in the past. This same pattern can be seen between the β-emitting radioisotopes in the Somerset Dam layered mafic intrusion radioisotopic data. The Rb-Sr whole-rock isochron "age" of 393±170 Ma (Figure 5) is older than the K-Ar whole-rock isochron "age" of 174±8 Ma (Figure 4), which is consistent with $^{87}$Rb having a longer half-life than $^{40}$K. However, the same pattern of isochron "ages" is not seen for the α-emitting radioisotopes in the Somerset Dam layered mafic intrusion. Further similar studies of suitable rock units are in progress in order to continue testing this suggested pattern in the effect of accelerated decay in the past on these radioisotope systems.

Finally, Snelling (2000) has extensively documented the role of geochemical processes in the earth's mantle and crust. These have resulted in the inheritance of radioisotopic ratios from the mantle and crustal magma sources of the intrusive and volcanic rocks now found at the earth's surface. From studies of present oceanic basalts it has been determined that Sr, Nd, and Pb isotopes can be used very effectively to identify the distinctive geochemistry of mantle reservoirs that were the sources of the magmas found today as basaltic oceanic crust and lavas on oceanic islands (Zingg, 1996). Because mafic rocks intruded into the earth's crust were also derived by partial melting of upper mantle sources, Sr, Nd, and Pb isotopes can similarly provide valuable information on the geochemical history of the mantle during the operation of past global tectonic processes.

Table 3 lists the relevant Sr, Nd, and Pb isotopic ratios for all 15 whole-rock samples of the macrolayers in the Somerset Dam layered gabbro intrusion. These are plotted on isotope correlation diagrams in Figure 8, which also show the isotopic characteristics of the defined mantle reservoirs (Rollinson, 1996). Also provided in Table 3 are the calculated epsilon Nd values, $\varepsilon_{Nd}(t_o)$, for the individual samples at the present day ($t_o$) compared to the present-day value of CHUR, the CHondrite Uniform Reservoir in the mantle (De Paolo & Wasserburg, 1976a; Rollinson). The magnitudes of the $\varepsilon_{Nd}$ ($t_o$) values reflect the degree of the time integrated depletion in Nd relative to CHUR. Additionally, Table 3 lists the calculated depleted mantle Nd model "ages" ($T_{DM}$) for each of the samples. These are calculated with reference to the present-day isotopic values for the depleted mantle (DM) reservoir from which the continental crust is regarded as having been largely extracted over time (De Paolo & Wasserburg, 1976b; Dickin, 1995; Rollinson).

The sample Nd and Sr isotopic ratios plotted in Figure 8(a) are identical to those obtained from the Somerset Dam layered mafic intrusion by Walker (1998). The depleted mantle (DM) region where most mid-ocean ridge basalts (MORBs) plot is connected to the bulk silicate earth (BSE) region by the mantle array along which most basalts from ocean islands, intra-oceanic island arcs and continents plot, including

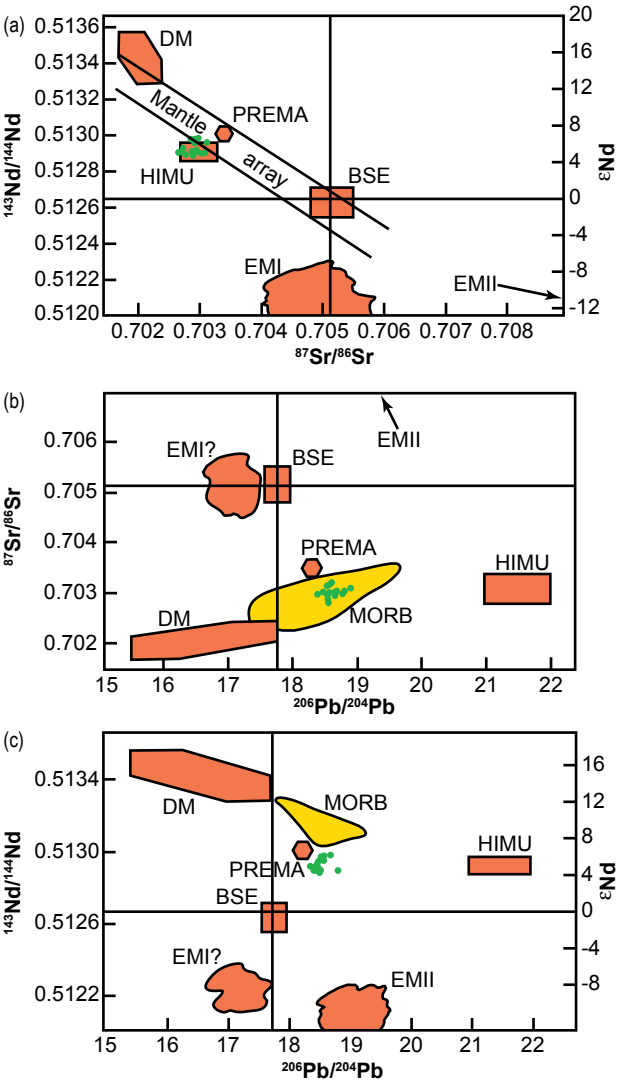


**Figure 8.** Isotope correlation diagrams on which are plotted all 15 samples from the Somerset Dam layered mafic intrusion (after Rollinson, 1996). The positions of the main oceanic mantle reservoirs identified by Zindler & Hart (1986) are shown: DM=depleted mantle, BSE=bulk silicate earth, EMI and EMII=enriched mantle I and II, HIMU=high mantle U/Pb ratio, PREMA=frequently observed PREvalent MAntle composition. (a) $^{143}$Nd/$^{144}$Nd versus $^{87}$Sr/$^{86}$Sr. The mantle array is defined by many oceanic basalts and a bulk earth value for $^{87}$Sr/$^{86}$Sr can be obtained from this trend. (b) $^{87}$Sr/$^{86}$Sr versus $^{206}$Pb/$^{204}$Pb. (c) $^{143}$Nd/$^{144}$Nd versus $^{206}$Pb/$^{204}$Pb. The yellow field is the mid-ocean ridge basalts (MORB). The $^{206}$Pb/$^{204}$Pb value of the bulk earth differs from that of Allegre, Lewin, & Dupre (1988).

mantle-plume-related continental flood basalts and hot-spot continental basalts (Rollinson, 1996). The gabbros from the Somerset Dam layered intrusion plot just outside and on the edge of the mantle array midway between the depleted mantle reservoir and the bulk silicate earth, within the mantle reservoir known as mantle with high U/Pb ratio (HIMU) and adjacent to the frequently observed prevalent mantle reservoir (PREMA). This indicates that the mantle source material from which partial melting produced the parental basaltic magma for the layered gabbro intrusion was already depleted by previous extraction of crustal magmatic materials. That is, the mantle source had already had a history of earlier extraction of basaltic magma by partial melting. Furthermore, there is no evidence of any significant crustal contamination of the parental basaltic magma to the Somerset Dam layered gabbros during its passage from its mantle source up into the upper continental crust.

In Figures 8(b) and (c) the Somerset Dam layered gabbros also plot in the general area of mantle depletion, again near the PREMA mantle reservoir, but this time in proximity to the MORB field rather than within the HIMU mantle reservoir. This is consistent with the conclusions drawn from Figure 8(a), namely, that the mantle source of the parental basaltic magma to the layered gabbros had already had a previous history of depletion via partial melting, and that the parental basaltic magma suffered negligible crustal contamination as it ascended from its mantle source up into the sub-volcanic magma chamber. Furthermore, the tight clustering of the data points throughout Figure 8 confirms that the parental basaltic magma for all the cyclic units in the Somerset Dam layered gabbro intrusion came from the same mantle source region.

Consistent with this evidence of a depleted mantle source for the parental basaltic magma are the depleted mantle Nd model "ages" ($T_{DM}$) of the gabbro macrolayers listed in Table 3. They generally range between 432.3 Ma and 700.5 Ma, but two oxide gabbro samples yield much greater "ages" of 1454.4 Ma and 2923.0 Ma. The depleted mantle Nd model "ages" are interpreted as the time in the past when the magma, that eventually formed the gabbros represented by the samples, was separated from the mantle reservoir (Rollinson, 1996). However, all the mineralogical, geochemical and other isotopic evidence points to the parental basaltic magma for all the cyclic units of the layered gabbro intrusion having been extracted from the same mantle source at the same time. If the layered gabbros' conventional "intrusion age" is 174±8 Ma, but the parental basaltic magma separated from its mantle source at, for example, 432.3 Ma, then does this imply that the magma required more than 250 million years to ascend from the mantle to the upper crust? Certainly not, if today's magma ascension rates of only years are any guide. Perhaps this vast spread of depleted mantle Nd model "ages" for these layered gabbros is further evidence of accelerated radioisotopic decay rates during the time the parental basaltic magma was being partially melted from its mantle source, and then ascending up into the upper crust and into the sub-volcanic magma chamber to form the layered intrusion.

However, if the postulated greater acceleration of $^{87}Rb$ decay compared to $^{40}K$ decay was proportional to the half-lives, then a corresponding acceleration of $^{147}Sm$ decay would also be expected to have occurred. The $^{147}Sm/^{40}K$ half-lives ratio is 83, while the $^{87}Rb/^{40}K$ half-lives ratio is 37. However, the Sm-Nd and K-Ar isochron "ages" are nearly equal (199±48 Ma compared with 174±8 Ma). The $^{147}Sm/^{87}Rb$ half-lives ratio is 2.2, yet the Sm-Nd isochron "age" (199±48 Ma) is only about half the Rb-Sr isochron "age" (393±170 Ma). On the other hand, the Pb-Pb isochron "age" of 1425±1000 Ma yields a similar range of "ages" (425–2425 Ma) to the depleted mantle Nd model "ages" (432.3–2923.0 Ma). Thus the Pb-Pb isochron "age" may be a radioisotopic/geochemical signature of the mantle source of the basaltic magma, that ascended to form the layered gabbro intrusion, similar to the depleted mantle Nd model "ages."

On this basis an alternative model for the radioisotopic "ages" of the Somerset Dam layered gabbro intrusion would be that the mantle source of the basaltic magma originally had K-Ar, Rb-Sr, Sm-Nd, and Pb-Pb radioisotopic ratios corresponding to "ages" within the 425–2425 Ma range. Such radioisotopic ratios could have been geochemical design features characteristic of the original primordial creation of the earth and its mantle, or of modifications made after initial creation of the earth as the mantle formed via differentiation (Baumgardner, 2000). Subsequently, during partial melting of the mantle source, and ascent and intrusion of the resultant basaltic magma, these radioisotopic ratios were perturbed, the K-Ar radioisotope system being affected the most because of Ar being an inert gas, while Rb-Sr ratios were affected less than Sm-Nd ratios.

Nevertheless, it is not inconsistent for accelerated nuclear decay to have provided the heat that powered the differentiation of the initially created earth into its core and mantle divisions and the subsequent development of the crust out of the mantle in the early part of the Creation week (Baumgardner, 2000). Such accelerated nuclear decay could have thus produced these geochemical design features of vast depleted mantle Nd model "ages" and the "age" spread in the Pb radioisotopes in the mantle source area from which the parental basaltic magma was later extracted by partial melting during the Flood

to produce the Somerset Dam gabbro intrusion with inherited radioisotopic arrays. Some additional minor accelerated nuclear decay during the Flood may have also contributed to the radioisotopic ratios now measured in the different gabbro macrolayers of this intrusion, particularly producing the discordances between the different radioisotope systems in the observed pattern as a result of the acceleration factor being proportional to the half-life of each radioisotopic system. Thus accelerated nuclear decay is the favored model for explaining the radioisotopic systematics found in this layered gabbro intrusion.

In any case, at the very least, it can be concluded that the Somerset Dam layered mafic intrusion has inherited the radioisotopic signature of its mantle source, and thus its present radioisotopic ratios do not provide the true age of the intrusion by the conventional radioisotopic dating techniques.

## Conclusions

Mineralogical, geochemical, and isotopic evidences all indicate that the cyclic units of gabbro macrolayers in the Somerset Dam layered mafic intrusion are coeval and were derived from the same parental basaltic magma. The original endowment of Ar, Sr, Nd, and Pb isotopes was homogeneously mixed, a necessary condition for successful conventional radioisotopic dating, particularly by the isochron method. However, the four analyzed radioisotope systems yield discordant whole-rock isochron "ages." The K-Ar radioisotope system produces an excellent 15-point isochron "age" of 174±8 Ma (Middle Jurassic), which should be regarded as the revised conventional age of this layered intrusion because the previously published "ages" that are discordant with it all rely on radioisotopic determinations on granitic rocks whose relationship to the layered gabbro intrusion is unclear. It is thus concluded that the discordances between these radioisotope systems in dating this same geologic event are likely due to changes in the decay rates of the different radioisotopic systems at some time or times in the past. It would also appear that of the β-emitting radioisotopes, $^{87}$Rb with its longer half-life yields an older "age" than $^{40}$K, suggesting $^{87}$Rb decay was accelerated more than $^{40}$K decay.

The Sr, Nd, and Pb isotopes also reveal that the parental basaltic magma of the Somerset Dam layered gabbro intrusion was partially melted from a depleted mantle source in a single episode, and that it suffered negligible crustal contamination as it ascended up and into the sub-volcanic magma chamber. However, the gabbros yield depleted mantle Nd model "ages" that supposedly indicate this separation from the mantle source by partial melting occurred hundreds of millions of years before the resultant basaltic magma formed the layered intrusion. This could be better explained by accelerated radioisotopic decay rates during partial melting and magma ascension. Nevertheless, it is concluded that the Somerset Dam layered mafic intrusion has inherited the radioisotopic signature of its mantle source, and thus its present radioisotopic ratios do not provide its true age by the conventional radioisotopic dating techniques.

## Acknowledgments

Initial work on this research was made possible by the logistical support of Answers in Genesis (Australia) for the first sample-collecting field trip, but the project has subsequently been fully supported by the Institute for Creation Research. Early help and discussions with Tas Walker are acknowledged, but all the work reported here is my own. All funding of the considerable cost of the whole-rock geochemical and radioisotopic analyses was provided by donors to the RATE (Radioisotopes and the Age of The Earth) project, whose contributions are gratefully acknowledged.

## References

Allegre, C.J., Lewin, E., & Dupre, B. (1988). A coherent crust-mantle model for the uranium-thorium-lead isotopic system. *Chemical Geology, 70*, 211–234.

Austin, S.A. (2000). Mineral isochron method applied as a test of the assumption of radioisotope dating. In L. Vardiman, A.A. Snelling, & E.F. Chaffin (Eds.), *Radioisotopes and the age of the earth: A young-earth creationist research initiative*, (pp. 95–121). El Cajon, California: Institute for Creation Research & St. Joseph, Missouri: Creation Research Society.

Baumgardner, J.R. (2000). Distribution of radioactive isotopes in the earth. In L. Vardiman, A.A. Snelling, & E.F. Chaffin (Eds.), *Radioisotopes and the age of the earth: A young-earth creationist research initiative*, (pp. 49–94). El Cajon, California: Institute for Creation Research & St. Joseph, Missouri: Creation Research Society.

Begemann, F., Ludwig, K.R., Lugmair, G.W., Min, K., Nyquist, L.E., Patchett, P.J., Renne, P.R., Shih, C.Y., Villa, I.N., & Walker, R.J. (2001). Call for improved set of decay constants for geochronological use. *Geochimica et Cosmochimica Acta, 65*, 111–121.

Cranfield, L.C., Schwartzbock, H., & Day, R.W. (1976). Geology of the Ipswich and Brisbane 1:250000 sheet areas. *Geological Survey of Queensland Report No. 95.*

Dalrymple, G.B. (1979). Critical tables for conversion of K-Ar Ages from old to new constants. *Geology, 7*, 558–560.

Dalrymple, G.B. & Lanphere, M.A. (1969). *Potassium-argon dating: Principles, techniques and applications to geochronology.* San Francisco: W.H. Freeman.

Day, R.W., Whittaker, W.G., Murray, C.G., Wilson, I.H., & Grimes, K.G. (1983). Queensland geology: A companion volume to the 1:2500000 scale geological map (1975). *Geological Survey of Queensland Publication 383.*

De Jersey, N.J. (1972). Triassic miospores from the Esk Beds. *Geological Survey of Queensland Publication 357, Palaeontological Papers, 32.*

De Jersey, N.J. (1973). Triassic miospores from the Bryden Formation. *Queensland Government Mining Journal, 74,*

377–378.

De Paolo, D.J. & Wasserburg, G.J. (1976a). Nd isotopic variations and petrogenetic models. *Geophysical Research Letters, 3*, 249–252.

De Paolo, D.J. & Wasserburg, G.J. (1976b). Inferences about magma sources and mantle structure from variations of $^{143}Nd/^{144}Nd$. *Geophysical Research Letters, 3*, 743–746.

Dickin, A.P. (1995). *Radiogenic isotope geology*. Cambridge, England: Cambridge University Press.

Ewart, A. & Grenfell, A. (1985). Cainozoic volcanic centres of south-eastern Queensland with special reference to the Main Range, Bunya Mountains and the volcanic centres of the Northern Brisbane Coastal Region. *Department of Geology University of Queensland papers, 11*(3), 1–57.

Flood, P.G. & Aitchison, J.C. (1993). Understanding new England geology: The comparative approach. In P.G. Flood & J.C. Aitchison (Eds.), *New England orogen, eastern Australia* (pp.1–10). Armidale, Australia: Department of Geology and Geophysics, University of New England.

Giem, P.A.L. (1997). *Scientific theology* (pp.144–146). Riverside, California: La Sierra University Press.

Hall, A. (1998). *Igneous petrology* (2nd ed.). Harlow, England: Addison Wesley Longman Ltd.

Harrington, H.J. & Korsch, R.J. (1985). Late Permian to Cainozoic tectonics of the New England Orogen. *Australian Journal of Earth Sciences, 32*, 181–203.

Irvine, P.N. (1982). Terminology for layered intrusions. *Journal of Petrology, 23*, 127–162.

Ludwig, K.R. (2001). *Isoplot/Ex (Version 2.49): The geochronological toolkit for Microsoft Excel*. University of California Berkeley, Berkeley Geochronology Center, Special Publication No.1a.

McBirney, A.R. & Noyes, R.M. (1979). Crystallization and layering of the Skaergaard Intrusion. *Journal of Petrology, 20*, 487–554.

Mathison, C.I. (1964). *Variation in the Somerset Dam layered basin complex*. Unpublished honours thesis. Department of Geology and Mineralogy, University of Queensland, Brisbane, Queensland, Australia.

Mathison, C.I. (1967). The Somerset Dam layered basic intrusion, south-eastern Queensland. *Journal of the Geological Society of Australia, 14*(1), 57–86.

Mathison, C.I. (1970). *The Somerset Dam Layered Basic Intrusion*. Unpublished Ph.D. thesis. University of Queensland, Brisbane, Queensland, Australia.

Mathison, C.I. (1975). Magnetites and ilmenites in the Somerset Dam layered basic intrusion, south-eastern Queensland. *Lithos, 8*, 93–111.

Mathison, C.I. (1987). Cyclic units in the Somerset Dam layered gabbro intrusion, south-eastern Queensland, Australia. *Lithos, 20*, 187–205.

McLeod, I.R. (1956). *The Somerset Igneous Complex*. Unpublished M.Sc. thesis. Department of Geology, University of Queensland, Brisbane, Queensland, Australia.

McLeod, I.R. (1959). The Somerset Dam igneous complex: A preliminary account. *University of Queensland paper, Department of Geology, 5*(3), 1–38.

Murphy, P.R., Schwarzbock, H., Cranfield, L.C., Withnall, I.W., & Murray, C.G. (1976). Geology of the Gympie 1:250000 Sheet Area. *Geological Survey of Queensland Report No. 96*.

Murphy, P.R., Trezise, D.L., Hutton, L.J., Cranfield, L.C, & Whitaker, W.G. (1979). *Caboolture sheet 9443 Queensland, 1:100000 Geological map series*. Geological Survey of Queensland, Brisbane.

Murphy, P.R., Trezise, D.L., Hutton, L.J., & Cranfield, L.C. (1987). 1:100000 *Geological Map commentary, Caboolture sheet 9443 Queensland*. Geological Survey of Queensland, Brisbane.

Ollier, C.D. (1982). The great escarpment of eastern Australia: Tectonic and geomorphic significance. *Journal of the Geological Society of Australia, 29*, 13–23.

Riley, C.M. (1991). *The Somerset Dam igneous complex*. Unpublished B.Sc. Honours thesis. Department of Applied Geology, Queensland University of Technology, Brisbane Queensland, Australia.

Rollinson, H.R. (1996). *Using geochemical data: Evaluation, presentation, interpretation*. Harlow, England: Addison Wesley Longman Ltd.

Snelling, A.A. (2000). Geochemical processes in the mantle and crust. In L. Vardiman, A.A. Snelling, & E.F. Chaffin (Eds.), *Radioisotopes and the age of the earth: A young-earth creationist research initiative* (pp.123–304). El Cajon, California: Institute for Creation Research & St. Joseph, Missouri: Creation Research Society.

Snelling, A.A., Austin, S.A., & Hoesch, W.A. (2003). Radioisotopes in the diabase sill (Upper Precambrian) Bass Rapids, Grand Canyon, Arizona: An application and test of the isochron dating method. In R.L. Ivey Jr. (Ed.), *Proceedings of the fifth international conference on creationism* (pp.269–284). Pittsburgh, Pennsylvania: Creation Science Fellowship.

Steiger, R.H. & Jäger, E. (1977). Subcommission on geochronology: Convention of the use of decay constants in geo- and cosmochronology. *Earth and Planetary Science Letters, 36*, 359–362.

Wager, L.R., Brown, G.M., & Wadsworth, W.J. (1960). Types of igneous cumulates. *Journal of Petrology, 1*, 73–85.

Wager, L.R. & Brown, G.M. (1968). *Layered igneous rocks*. Edinburgh: Oliver and Boyd.

Walker, T.B. (1998). *The Somerset Dam Igneous Complex, south-east Queensland*. Unpublished honours thesis B.Sc. Department of Earth Sciences, The University of Queensland, Brisbane, Queensland, Australia.

Walsh, J.J. (1972). *The geophysics and geology of the Somerset Dam basic layered intrusion of south-east Queensland, and the Mt Goondicum basic layered intrusion of the Monto District*. Unpublished honours thesis B.Sc. Department of Geology and Mineralogy, University of Queensland, Brisbane, Queensland, Australia.

Webb, A.W. & McDougall, I. (1967). Isotopic dating evidence on the age of the Upper Permian and Middle Triassic. *Earth and Planetary Science Letters, 2*, 483–488.

Webb, A.W., Stevens, N.C., & McDougall, I. (1967). Isotopic age determinations on Tertiary volcanic rocks and intrusives of south-eastern Queensland. *Proceedings of the Royal Society of Queensland, 79*, 79–92.

York, D. (1969). Least squares fitting of a straight line with correlated errors. *Earth and Planetary Science Letters, 5*, 320–324.

Zingg, A.J. (1996). Recystallization and the origin of layering in the Bushveld Complex. *Lithos, 37*, 15–37.

Zingler, A. & Hart, S.R. (1986). Chemical Geodynamics. *Annual Review of Earth and Planetary Sciences, 14*, 493–571.